

On the Mechanism of Interaction of Potent Surmountable and Insurmountable Antagonists with the Prostaglandin D₂ Receptor CRTH2[§]

Jesper Mosolff Mathiesen, Arthur Christopoulos, Trond Ulven, Julia F. Royer, Mercedes Campillo, Akos Heinemann, Leonardo Pardo, and Evi Kostenis

7TM Pharma A/S, Hørsholm, Denmark (J.M.M., E.K., T.U.); Department of Pharmacology, Monash University, Victoria, Australia (A.C.); Department of Experimental and Clinical Pharmacology, Medical University Graz, Graz, Austria (J.F.R., A.H.); Laboratorio de Medicina Computacional, Unidad de Bioestadística, Facultad de Medicina, Universidad Autónoma de Barcelona, Barcelona, Spain (M.C., L.P.); and Department of Chemistry, University of Southern Denmark, Odense, Denmark (T.U.)

Received August 8, 2005; accepted January 17, 2006

ABSTRACT

Chemoattractant receptor-homologous molecule expressed on T helper 2 cells (CRTH2) has attracted interest as a potential therapeutic target in inflammatory diseases. Ramatroban, a thromboxane A₂ receptor antagonist with clinical efficacy in allergic rhinitis, was recently found to also display potent CRTH2 antagonistic activity. Here, we present the pharmacological profile of three ramatroban analogs that differ chemically from ramatroban by either a single additional methyl group (TM30642), or an acetic acid instead of a propionic acid side chain (TM30643), or both modifications (TM30089). All three compounds bound to human CRTH2 stably expressed in human embryonic kidney 293 cells with nanomolar affinity. [³H]Prostaglandin D₂ (PGD₂) saturation analysis reveals that ramatroban and TM30642 decrease PGD₂ affinity, whereas TM30643 and TM30089 exclusively depress ligand binding capacity (B_{max}). Each of the three compounds acted as potent

CRTH2 antagonists, yet the nature of their antagonism differed markedly. In functional assays measuring inhibition of PGD₂-mediated 1) guanosine 5'-O-(3-thio)triphosphate binding, 2) β-arrestin translocation, and 3) shape change of human eosinophils endogenously expressing CRTH2, ramatroban, and TM30642 produced surmountable antagonism and parallel rightward shifts of the PGD₂ concentration-response curves. For TM30643 and TM30089, this shift was accompanied by a progressive reduction of maximal response. Binding analyses indicated that the functional insurmountability of TM30643 and TM30089 was probably related to long-lasting CRTH2 inhibition mediated via the orthosteric site of the receptor. A mechanistic understanding of insurmountability of CRTH2 antagonists could be fundamental for development of this novel class of anti-inflammatory drugs.

Prostaglandin D₂ (PGD₂) is the major prostanoid released by activated mast cells and is implicated as proinflammatory

This work was supported by the European Community's Sixth Framework Programme, Grant LSHB-CT-2003-503337.

Article, publication date, and citation information can be found at <http://molpharm.aspetjournals.org>.
doi:10.1124/mol.105.017681.

[§] The online version of this article (available at <http://molpharm.aspetjournals.org>) contains supplemental material.

mediator in diseases such as allergic rhinitis, atopic dermatitis, and asthma (Hata and Breyer, 2004). The prime mode of PGD₂ action is through two G protein-coupled receptors referred to as DP/DP1 and CRTH2/DP2, respectively (Boie et al., 1995; Hirai et al., 2001). Both PGD₂ receptors transduce extracellular signals predominantly by coupling to heterotrimeric G proteins. DP is positively linked to adenylyl cyclases via G_{α_s} proteins. CRTH2 negatively regulates adenylyl cy-

ABBREVIATIONS: PDG₂, prostaglandin D₂; DP, prostaglandin D receptor; CRTH2, chemoattractant receptor-homologous molecule expressed on T helper 2 cells; Th2, T helper 2; TM27868, 1-(4-ethoxyphenyl)-5-methoxy-2-methylindole-3-carboxylic acid; PCR, polymerase chain reaction; ELISA, enzyme-linked immunosorbent assay; β-arr2, β-arrestin2; βarr2-GFP², green fluorescent protein-β-arrestin2-(R393E, R395E) fusion protein; CRTH2-Rluc, *Renilla reniformis* luciferase-CRTH2 fusion protein; HEK, human embryonic kidney; BRET, bioluminescence resonance energy transfer; HBSS, Hanks' balanced salt solution; DMSO, dimethyl sulfoxide; BSA, bovine serum albumin; PBS, phosphate-buffered saline; GTPγS, guanosine 5'-O-(3-thio)triphosphate; PTX, pertussis toxin; EXP3174, 2-butyl-4-chloro-1-((2'-(1H-tetrazol-5-yl)(1,1'-biphenyl)-4-yl)methyl)-1H-imidazole-5-carboxylic acid; SC-54629, 1-(2,6-dimethylphenyl)-4-butyl-1,3-dihydro-3-((6-(2-(1H-tetrazol-5-yl)phenyl)-3-pyridinyl)methyl)-2H-imidazol-2-one; SC-54628, 1-(2-methylphenyl)-4-butyl-1,3-dihydro-3-((6-(2-(1H-tetrazol-5-yl)phenyl)-3-pyridinyl)methyl)-2H-imidazol-2-one; TM30642, 3-{3-[(4-fluoro-benzenesulfonyl)-methyl-amino]-1,2,3,4-tetrahydro-carbazol-9-yl}-propionic acid; TM30643, [3-(4-fluoro-benzenesulfonylamino)-1,2,3,4-tetrahydro-carbazol-9-yl]-acetic acid; TM30089, {3-[(4-fluoro-benzenesulfonyl)-methyl-amino]-1,2,3,4-tetrahydro-carbazol-9-yl}-acetic acid.

clases through $G\alpha_i$ proteins, mobilizes intracellular calcium, and stimulates phosphoinositide 3-kinase, mitogen-activated protein kinases and phospholipase C (Hata and Breyer, 2004). However recent in vitro studies have shown that CRTH2 can also signal via a G protein-independent, arrestin-dependent mechanism that is operative in human eosinophils (Mathiesen et al., 2005). CRTH2 is expressed on Th2 cells, eosinophils, basophils, and monocytes (Nagata et al., 1999; Powell, 2003; Hata and Breyer, 2004), cells that are all established contributors to allergic disease processes. In vitro, CRTH2 activation accounts for PGD₂-mediated Th2, eosinophil, and basophil chemotaxis (Hirai et al., 2001; Bohm et al., 2004), up-regulation of surface integrins (Monneret et al., 2003; Powell, 2003), secretion of prototypical Th2 cytokines such as interleukin-4, -5, and -13 and proinflammatory chemokines (Tanaka et al., 2004), and increased proliferative responses to T-cell receptor activation (Soler et al., 2005). In vivo, CRTH2 mediates eosinophil mobilization from the bone marrow (Heinemann et al., 2003) and their trafficking into the airways (Shiraishi et al., 2005). The genes encoding CRTH2 and DP have been disrupted individually and in combination by gene targeting (Gonzalo et al., 2005). That study revealed that CRTH2 but not DP is the predominant PGD₂ receptor involved in airway inflammation, mucus production, and airway hyper-responsiveness. Although a wealth of evidence suggests a significant proinflammatory role for CRTH2, its precise role in allergic diseases is not fully understood, in part because of the lack of appropriate inhibitors suitable for evaluation of the in vivo relevance of the PGD₂-CRTH2 relationship. The orally available small molecule ramatroban (Fig. 1), which was originally developed as a thromboxane A₂ receptor antagonist and is currently marketed in Japan for treatment of allergic rhinitis, has recently been shown to also antagonize CRTH2 with a potency sufficient to account at least in part for the beneficial clinical effects of ramatroban (Sugimoto et al., 2003; Robarge et al., 2005; Ulven and Kostenis, 2005). However, the inability of ramatroban to selectively inhibit one receptor to the exclusion of the other currently precludes our ability to draw any clear inferences from in vivo studies conducted with this molecule. Hence, potent and selective CRTH2 antagonists would be desirable to explore the involvement of PGD₂ and CRTH2 in allergic and atopic conditions.

Antagonists of G protein-coupled receptors can be distin-

guished as either surmountable or insurmountable (Lew et al., 2000; Vauquelin et al., 2002). Surmountable antagonists produce parallel rightward shifts of agonist concentration-response curves without altering the maximal agonist response. Insurmountable antagonists partially or completely decrease the maximal agonist response and may or may not induce concomitant rightward shifts of agonist dose-response curves. Insurmountable antagonism has been observed for a variety of GPCR systems, including those for angiotensin II, histamine, acetylcholine, serotonin, substance P, bradykinin, cysteinyl-leukotrienes, ADP, glutamate, and anaphylatoxin C5a (Schambye et al., 1994; Aramori et al., 1997; Lew et al., 2000; Carroll et al., 2001; Gillard et al., 2002; Vauquelin et al., 2002; Marteau et al., 2003; Rashid et al., 2003; March et al., 2004; Takezako et al., 2004). It is a priori unclear whether one type of antagonism is desired over the other to obtain clinical efficacy; nevertheless, insurmountable behavior of antagonists may be a means to obtain long-lasting receptor blockade in vivo.

We have previously reported the synthesis and selectivity profile of three novel ramatroban analogs (Fig. 1), which represented the first highly selective and potent CRTH2 antagonists (Ulven and Kostenis, 2005). In the current study, we present a detailed pharmacological analysis of their antagonistic profile, in comparison with ramatroban as a reference antagonist, using mammalian cells overexpressing CRTH2 or human eosinophils that naturally express CRTH2. Despite their close structural resemblance and similar binding affinities to CRTH2, the compounds display significant differences in the nature of their antagonism. Elucidation of the molecular mechanism underlying the divergent modes of CRTH2 blockade (surmountable versus insurmountable) of the compounds is presented. This is the first report disclosing both surmountable and insurmountable selective and potent antagonists for CRTH2 as valuable tools for further exploring the role of CRTH2 in vitro and in vivo.

Materials and Methods

Materials

White 96-well Optiplates and DeepBlueC were obtained from PerkinElmer Life and Analytical Sciences (Boston, MA). Tissue culture media and reagents were purchased from the Invitrogen (Breda, The Netherlands). PGD₂ was from Cayman Chemical (Ann Arbor, MI) and [³H]PGD₂ was from PerkinElmer Life and Analytical Sciences. TM27868 was obtained from ChemDiv (San Diego, CA). Eotaxin was from Preprotech EC (London, UK). CellFix and FACSFlow were from BD Immunocytometry Systems (Vienna, Austria). Fixative solution was prepared by diluting Cellfix 1:10 in distilled water and 1:4 in FACSFlow. Ramatroban was obtained from Bayer AG (Wuppertal, Germany). Synthesis of the CRTH2 antagonists TM30642, TM30643, and TM30089 was described previously (Ulven and Kostenis, 2005). All other laboratory reagents were from Sigma-Aldrich (St. Louis, MO), unless explicitly specified.

Generation/Origin of the cDNA Constructs

The coding sequence of human CRTH2 (GenBank accession no. NM_004778) was amplified by PCR from a human hippocampus cDNA library and inserted into the pcDNA3.1(+) expression vector (Invitrogen) via 5' HindIII and 3' EcoRI. To generate a CRTH2-*Renilla reniformis* luciferase (CRTH2-Rluc) fusion protein, the CRTH2 coding sequence without a STOP codon and Rluc were amplified, fused in frame by PCR, and subcloned into the pcDNA3.1(+)/Zeo expression vector. For ELISA experiments, the 78-

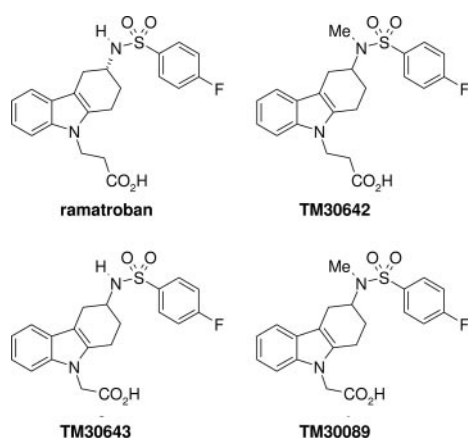


Fig. 1. Structures of ramatroban and its analogs TM30642, TM30643, and TM30089.

base pair M1 FLAG-epitope tag was introduced by PCR at the extreme N terminus, and the resulting construct was inserted via 5' NheI and 3' EcoRI into pcDNA3.1(+). Human β -arrestin2 (β -arr2) N-terminally tagged with GFP² (GFP²/ β -arr2) and *R. reniformis* luciferase were purchased from Packard BioSignal Inc. The β -arr2 mutant incapable of interacting with the endocytic machinery (β -arr2, R393E, R395E) was a generous gift from R. Jørgensen (7TM Pharma A/S, Hørsholm, Denmark) and has been described previously (Vrecl et al., 2004). The sequence identity of the constructs was verified by restriction endonuclease digests and sequencing in both directions on an ABI Prism 310 DNA sequencer (Applied Biosystems, Foster City, CA).

Cell Culture and Transfection

COS-7 cells were grown in Dulbecco's modified Eagle's medium 1885 supplemented with 10% fetal bovine serum and 10 μ g/ml gentamicin and kept at 37°C in a 10% CO₂ atmosphere. HEK293 cells were maintained in minimal essential medium supplemented with 10% (v/v) heat-inactivated fetal calf serum, 2 mM GlutaMAX-I, 1% nonessential amino acids, 1% sodium pyruvate, and 10 μ g/ml gentamicin. For functional inositol phosphate assays, COS-7 cells were transiently cotransfected with CRTH2 and a promiscuous G α protein facilitating inositol phosphate production by the G_i-selective CRTH2 receptor (Kostenis et al., 2005) using a calcium phosphate-DNA coprecipitation method with the addition of chloroquine (Mathiesen et al., 2005). To perform the functional bioluminescence resonance energy transfer (BRET) assays, a HEK293 cell clone stably expressing β arr2-R393E, R395E-GFP², and CRTH2-Rluc was generated. This cell line will hereafter be referred to as CRTH2-HEK293 stable cells.

Binding Experiments

Whole Cell Binding. CRTH2-HEK293 cells were seeded into 96-well plates at a density of 30,000 cells/well. Competition binding experiments on whole cells were then performed approximately 18 to 24 h later using 1.2 nM [³H]PGD2 (172 Ci/mmol; NEN) in a binding buffer consisting of HBSS (Invitrogen) and 10 mM HEPES, pH 7.4. Competing ligands were diluted in DMSO, which was kept constant at 1% (v/v) of the final incubation volume. Total and nonspecific binding were determined in the absence and presence of 10 μ M PGD2. Binding reactions were routinely conducted for 3 h at 4°C and terminated by two washes (100 μ l each) with ice-cold binding buffer. Radioactivity was determined by liquid scintillation counting in a TopCount liquid scintillation counter (PerkinElmer Life and Analytical Sciences) after overnight incubation in MicroScint 20. For saturation binding experiments, CRTH2-HEK293 cells were incubated with 1.5 to 48 nM [³H]PGD2 for 3 h in the absence and presence of equivalent concentrations (with respect to receptor occupancy) of CRTH2 antagonists, and nonspecific binding determined in the presence of 10 μ M PGD2. The exact concentration of [³H]PGD2 used was determined from experiment to experiment. Determinations were made in duplicates.

Dissociation Kinetics. CRTH2-HEK293 whole cells (250,000 cells/ml) were incubated at 4°C with 3 nM [³H]PGD2 in binding buffer (HBSS + 10 mM HEPES, pH 7.4) for 60 min to obtain equilibrium. Dissociation was initiated by adding 10 μ M PGD2 alone or in combination with 20 μ M CRTH2 antagonists ramatroban, TM30089, or TM27868, respectively. After various time intervals, 200- μ l aliquot samples were taken, and the reaction was terminated by sample filtration on a Millipore vacuum manifold using Whatman GF/F filters (presoaked in 0.5% BSA for at least 1 h). The filters were washed rapidly three times with 3 ml of ice-cold binding buffer, and radioactivity was determined in a beta counter (PerkinElmer Life and Analytical Sciences). In a separate set of dissociation kinetics, dissociation was initiated with an excess of PGD2 (10 μ M), ramatroban (20 μ M), or TM30089 (20 μ M) alone.

Association Kinetics. The rate of [³H]PGD2 binding to CRTH2 receptors in whole CRTH2-HEK293 cells at 4°C was measured after preincubation with vehicle (DMSO) or equivalent concentrations of CRTH2 antagonists ($K_i \times 10$) for 30 min. CRTH2-HEK293 whole cells were preincubated with antagonists or vehicle for 30 min, washed in 10 ml of binding buffer to remove nonbound antagonist, and resuspended, followed by addition of 4 nM [³H]PGD2 to initiate association using 500,000 cells/ml. After various time intervals, 200- μ l aliquot samples (100,000 cells) were taken and processed as described under *Dissociation Kinetics*. Binding equilibrium was reached after 60 min at 4°C.

BRET² Assay

Functional BRET² (hereafter referred to as BRET) assays were performed on HEK293 cells stably expressing human CRTH2-Rluc and GFP²- β -arr2, R393E, R395E essentially as described previously (Vrecl et al., 2004). Before the assay, cells were detached and resuspended in Dulbecco's PBS with 1000 mg/l L-glucose at a density of 2×10^6 cells/ml. DeepBlueC was diluted to 50 μ M in Dulbecco's PBS with 1000 mg/l L-glucose (light sensitive). Cell suspension (100 μ l) was transferred to wells in a 96-well microplate (white OptiPlate) and placed in the Mithras LB 940 instrument (Berthold Technologies, Bad Wildbad, Germany). Agonist (12 μ l/well) was then injected by injector 1, and 10 μ l/well DeepBlueC was injected simultaneously by injector 2. Five seconds after the injections, the light output from the well was measured sequentially at 400 and 515 nm, and the BRET signal [milliBRET (mBRET) ratio] was calculated by the ratio of the fluorescence emitted by GFP²- β -arr2 (515 nm) over the light emitted by the receptor-Rluc (400 nm). Antagonists were preincubated with the cells for 15 min before the addition of agonist and DeepBlueC. Compounds were dissolved in DMSO, and the final DMSO concentration was kept constant at 1% in the assay. For BRET experiments in the presence of pertussis toxin, cells were incubated overnight in the presence of the toxin at a final concentration of 100 ng/ml. Use of the BRET² assay and the GFP²- β -arr2, R393E, R395E mutant for BRET² requires a license from 7TM Pharma A/S.

[³⁵S]GTP γ S Binding Assays

Scintillation proximity assay [³⁵S]GTP γ S binding was performed on membranes from CHO-K1 cells stably expressing CRTH2 essentially as described in Mathiesen et al. (2005). Four micrograms of membrane protein was incubated in GTP γ S binding buffer (50 mM HEPES, pH 7.5, 100 mM NaCl, 5 mM MgCl₂, 0.1% BSA, and 10 μ g/ml saponin) with 50 nCi of [³⁵S]GTP γ S, 1 μ M GDP, and 0.4 mg of wheat germ agglutinin-coupled scintillation proximity assay beads (RPNQ0001; GE Healthcare, Little Chalfont, Buckinghamshire, UK) with or without increasing concentrations of PGD2 in the absence or presence of the various CRTH2 antagonists. Parallel assays containing 100 μ M nonradioactive GTP γ S defined nonspecific binding. Samples were incubated for 30 min at ambient temperature on a plate shaker, centrifuged for 5 min, and radioactivity was counted in a TopCount liquid scintillation counter.

Inositol Phosphate Accumulation Assays

Twenty-four hours after transfection cells were seeded in 24-well tissue culture plates and loaded with 5 μ Ci of [2-³H]myo-inositol (TRK911; Amersham Biosciences). The next day, cells were washed twice in HBSS buffer (including CaCl₂ and MgCl₂; Invitrogen) and stimulated with the respective agonists in HBSS buffer supplemented with 5 mM LiCl for 45 min at 37°C. Antagonists are routinely preincubated for 15 min before the 45-min agonist incubation period. The reactions were terminated by aspiration and addition of 10 mM ice-cold formic acid and incubated for 30 min on ice. The lysate was applied to AG 1-X8 anion exchange resin (Bio-Rad, Hercules, CA) and washed twice with buffer containing 60 mM sodium formate and 5 mM borax. The [³H]inositol phosphate fraction was

then eluted by adding 1 M ammonium formate and 100 mM formic acid solution and counted after addition of HiSafe3 scintillation fluid (PerkinElmer Life and Analytical Sciences).

Enzyme-Linked Immunosorbent Assay

Determination of cell surface expression levels of CRTH2 was performed using an N-terminally FLAG-tagged CRTH2 receptor in an ELISA assay as described previously (Mathiesen et al., 2005). Twenty-four hours after transfection cells were seeded in poly-D-lysine-coated 48-well tissue culture plates at a density of 100,000 cells/well. Approximately 48 h after transfection, cells were washed once in minimal essential medium + 0.1% BSA and exposed to the indicated compounds diluted in the same buffer for 30 or 180 min at both 37 and 4°C. Cells were then fixed with 4% paraformaldehyde, and CRTH2 surface expression levels were determined with the 3,3',5,5'-tetramethylbenzidine (Sigma-Aldrich) substrate. All experiments were performed in triplicate determinations.

Human Eosinophil Shape Change Assay

Blood was sampled from healthy volunteers according to a protocol approved by the Ethics Committee of the University of Graz and processed as described previously (Bohm et al., 2004). Preparations of polymorphonuclear leukocytes (containing eosinophils and neutrophils) were prepared by dextran sedimentation of citrated whole blood and Histopaque gradients. The resulting cells were washed and resuspended in assay buffer (comprising PBS with $\text{Ca}^{2+}/\text{Mg}^{2+}$ supplemented with 0.1% BSA, 10 mM HEPES, and 10 mM glucose, pH 7.4) at 5×10^6 cells/ml. Cells were incubated with the antagonists or vehicle (PBS or DMSO) for 10 min at 37°C and then stimulated with various concentrations of the agonists (PGD2 or eotaxin) for 4 min at 37°C. To stop the reaction, samples were transferred to ice and fixed with 250 μl of fixative solution. Samples were immediately analyzed on a FACSCalibur flow cytometer (BD Biosciences), and eosinophils were identified according to their autofluorescence in the FL-1 and FL-2 channels. Shape change responses were quantified as percentage of the maximal response to PGD2 or eotaxin in the absence of an antagonist.

Calculations and Data Analysis

Analysis was performed using Prism 4.03 (GraphPad Software Inc., San Diego, CA). Data sets of saturation binding isotherms were analyzed via nonlinear regression according to a hyperbolic, one-site binding model, and individual estimates for total receptor number (B_{max}) and radioligand dissociation constant (K_A) were calculated. The following equation was used:

$$Y = \frac{B_{\text{max}} \cdot [A]}{K_A + [A]} \quad (1)$$

where [A] denotes the concentration of radioligand, and B_{max} and K_A denote the true PGD₂ binding capacity and affinity, respectively.

Specific binding data from the [³H]PGD₂ competition binding assays using the test antagonists were normalized and fitted to the following empirical one-site model for competitive interaction:

$$Y = \text{Bottom} + \frac{(\text{Top} - \text{Bottom})}{1 + \frac{[B]}{K_B \left(1 + \frac{[A]}{K_A}\right)}} \quad (2)$$

where Y denotes percentage of specific binding, Top denotes maximal asymptotic binding, Bottom denotes the minimal asymptotic binding, [A] denotes the concentration of radioligand, [B] denotes the concentration of inhibitor, and K_A and K_B denote their respective equilibrium dissociation constants.

Data sets of [³H]PGD₂ homologous competition binding experiments (total binding), performed in the absence or presence of increasing concentrations of each test antagonist, were initially glo-

bally fitted to the following model for simple homologous competition:

$$Y = \frac{B_{\text{max}} \cdot [A_{\text{Hot}}]}{[A_{\text{Hot}}] + [A_{\text{Cold}}] + K_A} + \text{NS} \quad (3)$$

where B_{max} denotes the apparent maximal density of binding sites, K_A denotes the apparent equilibrium dissociation constant of PGD₂, $[A_{\text{Hot}}]$ denotes the concentration of radioligand, $[A_{\text{Cold}}]$ denotes the concentration of unlabeled PGD₂ (the independent variable), and NS denotes the fraction of nonspecific binding (Motulsky and Christopoulos, 2004). Note that the estimates of B_{max} and K_A are only estimates of true PGD₂ binding capacity and affinity, respectively, for the control curve in the absence of added antagonist. Subsequent to this fit, an F-test was used to determine whether the data could be better fitted by sharing the B_{max} and estimating a separate K_A for each curve (consistent with the expectations of competitive antagonism) or by sharing the K_A across the curves and estimating a separate B_{max} for each curve (indicative of noncompetitive antagonism; see Fig. 4 under *Results* for example). Data sets that were better described by assuming no change in B_{max} with increasing antagonist concentrations were then globally fitted to the following homologous binding model, which explicitly describes a surmountable competitive interaction between radioligand, homologous displacer and a second antagonist:

$$Y = \frac{B_{\text{max}} \cdot [A_{\text{Hot}}]}{[A_{\text{Hot}}] + [A_{\text{Cold}}] + K_A \left(1 + \frac{[B]}{K_B}\right)} + \text{NS} \quad (4)$$

where [B] denotes the concentration of second antagonist, K_B denotes its equilibrium dissociation constant, and all other parameters are as described above. In contrast, data sets that were better described by assuming no change in K_A with increasing antagonist concentrations were then globally fitted to the following homologous binding model, which explicitly describes an insurmountable noncompetitive interaction between radioligand, homologous displacer and a second antagonist

$$Y = \frac{B_{\text{max}} \cdot \left(\frac{K_B}{[B] + K_B}\right) \cdot [A_{\text{Hot}}]}{[A_{\text{Hot}}] + [A_{\text{Cold}}] + K_A} + \text{NS} \quad (5)$$

Functional concentration-response curves for PGD₂ obtained in the absence or presence of CRTH2 antagonists were fitted via nonlinear regression analysis to the following four-parameter logistic equation:

$$Y = \frac{(\text{Top} - \text{Bottom})}{1 + 10^{(\log(\text{EC}_{50}) - \log([A]))_{n_H}}} + \text{Bottom} \quad (6)$$

where Top denotes maximal asymptotic binding, Bottom denotes the minimal asymptotic binding, [A] denotes the concentration of radioligand, and n_H is the Hill coefficient. EC_{50} values were obtained as a measure of agonist potency and represent the effective concentrations of half-maximal responses.

pA_2 values were estimated from dose ratios (DR) calculated from the EC_{50} values of the individual dose response curves obtained in the absence ($\text{EC}_{50, \text{agonist alone}}$) and presence ($\text{EC}_{50, + [B]}$) of CRTH2 antagonists by fitting to the following equation using linear regression:

$$\log\left(\frac{\text{EC}_{50, + [B]}}{\text{EC}_{50, \text{agonist alone}}}\right) = \log([B]) - \log(K_B) \quad (7)$$

where [B] denotes the antagonist concentration used when estimating the EC_{50} for the agonist, and K_B is the dissociation constant of the antagonist. pA_2 was estimated as the interception of the regression line with the x-axis.

Data from association and dissociation kinetic experiments were analyzed to calculate the dissociation rate constants (K_{-1}) and the

observed association rate constants (K_{app}). To determine the dissociation rate constants of PGD2, data were fitted by nonlinear regression to the following equation:

$$Y = Y_{max} \cdot e^{-K_{-1} \cdot t} \quad (8)$$

where K_{-1} is the dissociation rate constant, and Y_{max} denotes the amount of specific binding at 0 min.

To determine the apparent association rate constant of PGD2 data were fitted by nonlinear regression to the following equation representing a biphasic association process:

$$Y = Y_{max1} \cdot (1 - e^{-K_{app1} \cdot t}) + Y_{max2} \cdot (1 - e^{-K_{app2} \cdot t}) \quad (9)$$

where the curve ascends to $Y_{max1} + Y_{max2}$ via a biphasic exponential association; K_{app1} and K_{app2} denote the individual apparent association rate constants.

In practice, all estimates of ligand potency or affinity were obtained as logarithms.

Results

The Tetrahydrocarbazoles TM30642, TM30643, and TM30089 Are Almost Equipotent Inhibitors of [³H]PGD2 Binding at Human CRTH2 Receptors

At the outset, ramatroban and the three analogs were tested for their ability to compete for [³H]PGD2 specific binding to human CRTH2 receptors stably expressed in HEK293 cells (CRTH2-HEK293 cells). All three compounds displaced [³H]PGD2-specific binding concentration dependently (Fig. 2) with estimated antagonist dissociation constants as shown in Table 1. The affinity of the reference antagonist ramatroban as determined in this set of assays is congruent with previously reported data (Sugimoto et al., 2003; Ulven and Kostenis, 2005; Fig. 2). To characterize the effects of the compounds on [³H]PGD2 binding in more detail, [³H]PGD2 saturation isotherms were generated in the absence and presence of equivalent concentrations (with respect to receptor occupancy) of inhibitor compounds (approx. $3 \times K_i$) (Fig. 3A). Compounds interacting with a receptor in a competitive and reversible manner alter radioligand affinity without affecting ligand binding capacity (B_{max}). Conversely, compounds interacting in a noncompetitive, slowly reversible or irreversible manner reduce binding capacity but have minimal, or no, effect on the affinity of the radiotracer. In the absence of competitor compounds, [³H]PGD2 binding to CRTH2-HEK293 whole cells was saturable, and data were fitted adequately to a one-site binding model [eq. 1; equilib-

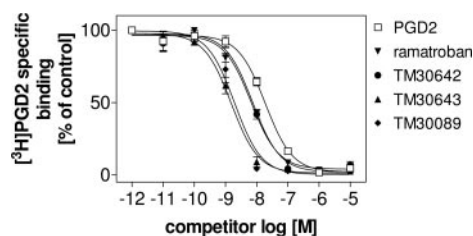


Fig. 2. Affinities of ramatroban and the three analogs TM30642, TM30643, and TM30089 for the cloned human CRTH2 receptor stably expressed in HEK293 cells (CRTH2-HEK293 cells). CRTH2-HEK293 whole cells were incubated at 4°C for 3 h with increasing concentrations of the competitor compounds. Nonspecific binding was defined in the presence of 10 μ M PGD2. K_i values were calculated by transforming the IC_{50} values according to the Cheng-Prusoff equation as described under *Materials and Methods*. Symbols represent the mean \pm S.E. of three independent experiments conducted in duplicate.

rium dissociation constant (K_D) and B_{max} values amounted to $K_D = 11.1 \pm 2.7$ nM, $B_{max} = 3.1 \pm 0.6$ pmol/mg]. To better visualize the apparent effects of the compounds on [³H]PGD2 affinity and receptor number, Scatchard plots were derived from the saturation isotherms (Fig. 3B). In the presence of ramatroban and its *N*-methylated analog TM30642 the affinity of [³H]PGD2 seemed to decrease as indicated by flatter slopes of the Scatchard regression lines, whereas B_{max} values remained unaffected as shown by similar interceptions of regression lines with the *x*-axis (Fig. 3B). In contrast, incubation of CRTH2-HEK293 cells with TM30643 and TM30089, in which the side chain linking the tetrahydrocarbazole scaffold with the carboxylic acid moiety is shortened by one methylene unit, seemed to decrease the number of PGD2 binding sites but did not alter PGD2 affinity.

Although saturation binding experiments and Scatchard analysis indicated a reduced [³H]PGD2 binding capacity in the presence of TM30643 and TM30089, a rigorous test of this assumption would have required a larger range of antagonist concentrations, and, as a consequence, appreciably larger (and practically unobtainable) tracer concentrations. In an attempt to circumvent this limitation but retain an ability to reliably quantify antagonist effects on radioligand binding affinity versus binding capacity, we developed a novel analytical method that is described in detail under *Materials and Methods*. To this end, a series of [³H]PGD2 homologous competition binding experiments were performed in the absence and presence of increasing concentrations of the respective CRTH2 antagonists. As shown in Fig. 4, a global analysis of the data according to eq. 3 under *Materials and Methods*, followed by F-test, revealed that the interaction between PGD2 and either ramatroban or TM30642 was best fitted by a model that assumed a change in the apparent affinity of PGD2 with no change in PGD2 B_{max} ; a single best-estimate of the latter parameter was able to describe all the curves in the data set for each antagonist. This behavior is consistent with simple surmountable antagonism. In contrast, application of the same test to the data measuring the interaction between PGD2 and either TM0643 or TM30089 revealed that the entire family of curves could best be fitted by assuming no change in PGD2 affinity (described by a single estimate for $\log K_A$) but a progressive reduction in B_{max} with increasing antagonist concentra-

TABLE 1

Antagonist potency estimates ($-\log K_B$ values) for indole CRTH2 antagonists determined from radioligand binding assays

Values are the mean of three to five independent experiments performed in duplicate. Unpaired *t* tests showed that TM30643 and TM30089 had significantly higher affinity to the receptor than ramatroban and 30642, respectively ($p < 0.01$) in both radioligand binding assays.

Compound	Assay	
	[³ H]PGD2 Inhibition Binding	[³ H]PGD2 Homologous Competition Binding
Ramatroban	8.19 \pm 0.06 ^a	8.13 \pm 0.01 ^b
TM30642	8.15 \pm 0.07 ^a	8.35 \pm 0.03 ^b
TM30643	8.85 \pm 0.06 ^a	8.89 \pm 0.04 ^c
TM30089	8.74 \pm 0.09 ^a	8.93 \pm 0.05 ^c

^a Parameter estimates represent the negative logarithm of the antagonist dissociation constant, derived by nonlinear regression analysis according to a competitive model (eq. 2).

^b Negative logarithm of the antagonist dissociation constant, derived by global nonlinear regression analysis according to a competitive binding model (eq. 4).

^c Negative logarithm of the antagonist dissociation constant, derived by global nonlinear regression analysis according to a noncompetitive binding model (eq. 5).

tion—behavior that is consistent with insurmountable antagonism. As a consequence, the ramatroban and TM30642 data sets were refitted to eq. 4 under *Materials and Methods*, which is based on a competitive model of interaction, to explicitly estimate the dissociation constant for either antagonist when interacting with PGD2; the resulting values are shown in Table 1. In contrast, the TM0643 or TM30089 data sets were globally refitted to eq. 5 under *Materials and Methods*, which is based on the standard model for noncompetitive antagonism. The estimated affinity values for these latter two antagonists are also shown in Table 1. It is noteworthy that a comparison of the antagonist affinity estimates obtained by this approach with those obtained by the more traditional inhibition binding method (Fig. 2), which assumes a strictly competitive, surmountable antagonism between ligands, yielded very similar values. An explanation as

to why this may be so is outlined under *Discussion* and the Appendix. Together, the inhibition and saturation binding experiments revealed that the tetrahydrocarbazole CRTH2 antagonists display similar receptor binding affinities but belong to two different pharmacological classes (i.e., surmountable and insurmountable antagonists).

Effects of the Compounds on PGD2-Mediated Responses in Different Functional Assays in Mammalian Cells, Overexpressing CRTH2

To determine the functional consequences of the divergent effects on [³H]PGD2 binding, concentration-dependent inhibition of PGD2 responses by the CRTH2 antagonists was evaluated in a set of different functional assays. We were particularly curious about the nature of antagonism of TM30643 and TM30089, because both compounds clearly

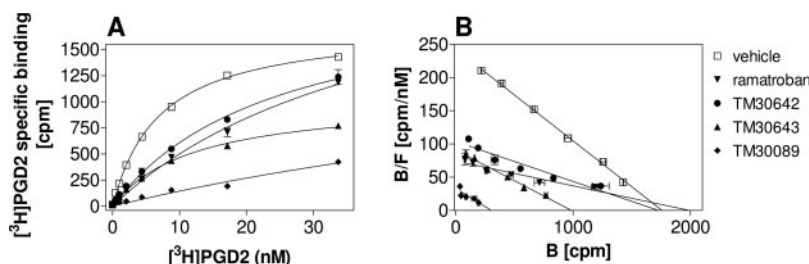


Fig. 3. Effect of ramatroban, TM30642, TM30643, and TM30089 on [³H]PGD2 saturation binding in CRTH2-HEK293 cells. A, representative saturation analysis of [³H]PGD2 binding to CRTH2 receptors in whole cells in the absence or presence of equivalent concentrations (with respect to receptor occupancy) of the compounds. Concentrations of compounds chosen inhibited approximately 75% of [³H]PGD2 specific binding at equilibrium (approximately $30 \times K_i$; see Fig. 2). Data were fitted best to a one-binding site model, and K_D and B_{max} values were determined. B, Scatchard transformation of the saturation isotherms shown in A. TM30643 and TM30089 significantly lowered B_{max} ($p < 0.05$) compared with vehicle- and ramatroban/TM30642-treated cells. [³H]PGD2 K_D values were significantly higher ($p < 0.05$) in the presence of ramatroban and TM30642 compared with vehicle-treated cells.

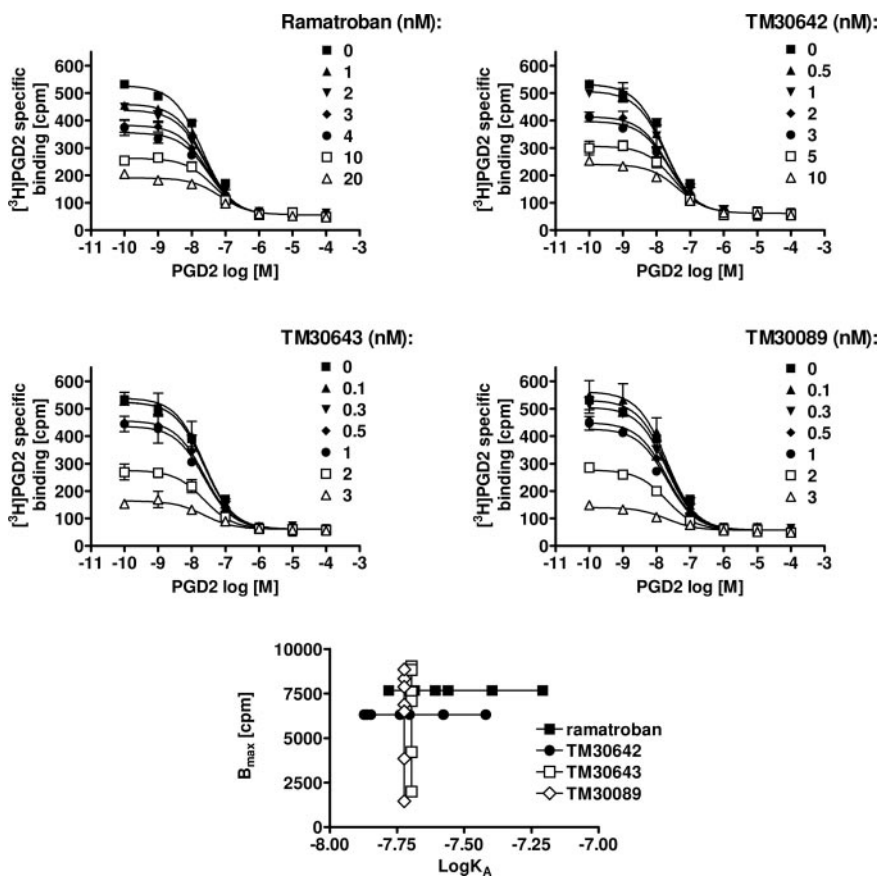


Fig. 4. Homologous competition binding between [³H]PGD2 (1.2 nM) and unlabeled PGD2 in the absence or presence of the indicated concentrations of CRTH2 antagonist. The data for ramatroban and TM30642 represent the best global fit according to a competitive binding model where the effect of each antagonist is to reduce the apparent binding affinity of PGD2 with no effect on the B_{max} (as determined by F-test). The data for TM30643 and TM30089 represent the best global fit according to a noncompetitive binding model, where the effect of each antagonist is to reduce the B_{max} of PGD2 with no effect on its binding affinity (as determined by F-test). Also shown is the relationship between the best-fit values for apparent B_{max} and $\text{log}K_A$ for each data set. Data shown are representative of a single experiment, performed in duplicate, which was repeated five times.

reduced the available number of PGD₂ sites on the cell surface, which may correlate to insurmountable inhibition of agonist responses in functional assays. First, the compounds were tested for their ability to antagonize PGD₂-mediated stimulation of [³⁵S]GTP γ S binding in membrane preparations from stably transfected CRTH2 cells (Fig. 5). Ramatroban and TM30642 caused parallel rightward shifts of the PGD₂ concentration-response curves without altering the maximal PGD₂ response, consistent with competitive and reversible antagonism. Estimated pA_2 values and slopes of the Schild regressions amounted to $pA_2 = 7.44 \pm 0.14$, $n_H = 0.91 \pm 0.05$ ($n = 5$) for ramatroban, and $pA_2 = 7.72 \pm 0.13$, $n_H = 0.89 \pm 0.075$ ($n = 3$) for TM30642, respectively. In contrast, TM30089 simultaneously shifted the PGD₂ dose-response curve to the right and decreased the maximal PGD₂ response, indicating insurmountable antagonism. TM30643 induced clear rightward shifts of PGD₂ concentration-effect curves in concentrations up to 1 μ M; at a concentration of 10 μ M, however, E_{max} of PGD₂ seemed to be depressed. A pA_2 value for TM30643 was computed excluding the PGD₂ dose-response curve in the presence of the highest applied concen-

tration of TM30643 and amounted to $pA_2 = 8.37 \pm 0.08$, $n_H = 1.06 \pm 0.02$ ($n = 3$).

Very similar pharmacological profiles of the antagonists were obtained when inhibition of PGD₂-stimulated inositol phosphate production (Supplemental Fig. 1) or β -arrestin translocation was measured (Fig. 6). It is noteworthy that the level of attenuation of maximal PGD₂ responses was greater in inositol phosphate and β -arrestin translocation assays (Fig. 6) compared with GTP γ S assays (Fig. 5), which may relate to the lower level of CRTH2 receptor expression in the former two assays ($B_{max} = 3.1$ versus 10.2 pmol/mg protein). None of the compounds showed any significant stimulatory effect in the various functional assays (Supplemental Fig. 2). Together, the functional data reveal that TM30642 and ramatroban exhibit surmountable inhibition of PGD₂ responses, whereas TM30089 and to a lesser extent TM30643 clearly display insurmountable antagonism.

We have recently shown that CRTH2-mediated β -arrestin recruitment has a major G protein-independent component and is uncoupled from $G\alpha_{i/o}$ activation in HEK293 cells (Mathiesen et al., 2005). To test whether the set of CRTH2 antagonists retains its pharmacological profile when β -arrestin recruitment is exclusively mediated in a G protein-inde-

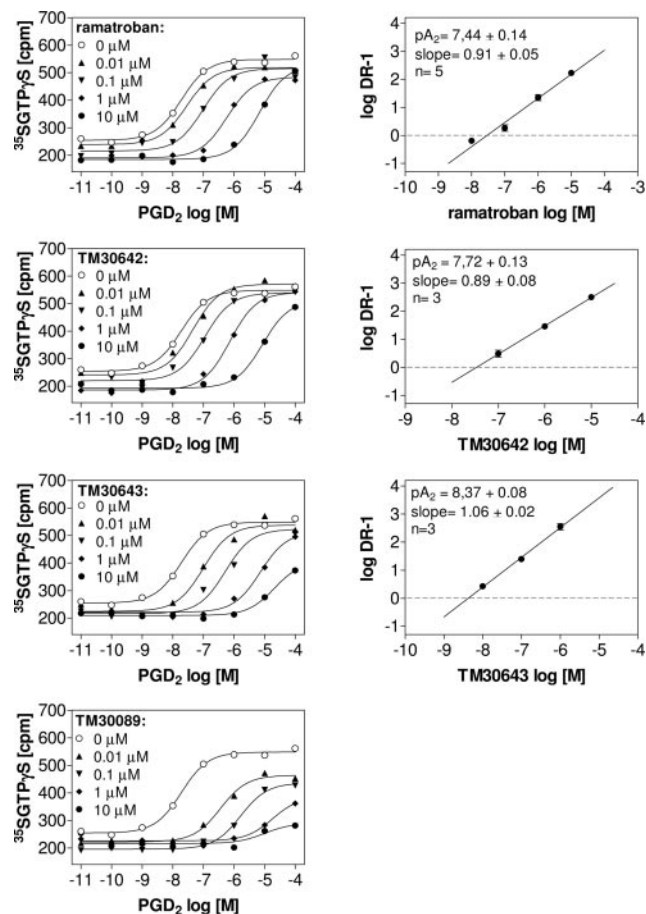


Fig. 5. Effects of ramatroban, TM30642, TM30643, and TM30089 on PGD₂-mediated stimulation of [³⁵S]GTP γ S binding in Chinese hamster ovary cell membranes stably expressing human CRTH2. PGD₂ dose-response curves were performed in the presence of the indicated concentrations of the compounds (left) and dose ratios were transformed into Schild plots (right). The plots of the dose ratios over antagonist concentration were subjected to linear regression analysis, and pA_2 values were determined as the x -intercepts at $\log(DR - 1) = 0$. Data are means \pm S.D. of one of three representative experiments each performed in duplicate.

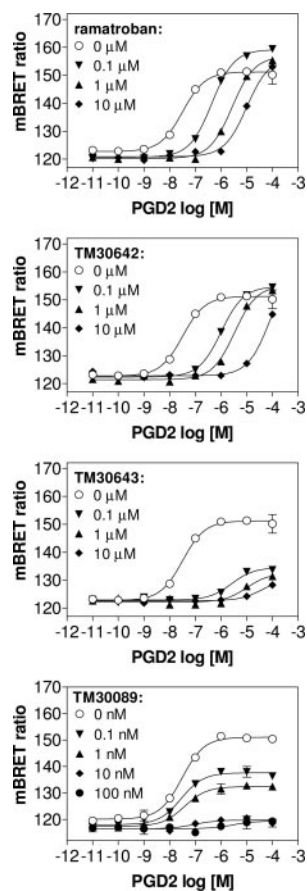


Fig. 6. Effects of ramatroban, TM30642, TM30643, and TM30089 on PGD₂-mediated stimulation of β -arrestin recruitment by CRTH2 in BRET assays. HEK293 cells stably transfected with a modified β -arrestin-GFP² and CRTH2-Rluc (for details, see *Materials and Methods*) were preincubated for 15 min at 37°C with fixed concentrations of the compounds before arrestin translocation was initiated by addition of increasing concentrations of PGD₂. mBRET ratios were calculated as described under *Materials and Methods*. Shown are means \pm S.D. of one of three independent experiments, each performed in duplicate.

pendent manner, CRTH2-expressing cells were pretreated with PTX, a selective inhibitor of $G\alpha_{i/o}$ proteins. PTX treatment decreased PGD₂-mediated arrestin recruitment in CRTH2-HEK293 cells by approximately 20%, confirming the substantial $G\alpha_i$ -independent component. However, the nature of antagonism of the compounds was essentially unchanged in PTX-treated cells (Supplemental Fig. 3), suggesting that the nature of antagonism is independent of the cellular signaling pathway used by CRTH2.

The Compounds Preserve Their Pharmacological Profile in Human Eosinophils, Naturally Expressing CRTH2

It is well known that insurmountable antagonism not only depends on the level of receptor expression in a given tissue or cell but also may differ depending on the cellular environment of a given receptor. We therefore analyzed antagonist behavior in a more natural ex vivo cell system, using human eosinophils, which endogenously express CRTH2 as a model system. Purified human eosinophils undergo shape change upon exposure to PGD₂ that is characterized by a biphasic dose-response curve (Hirai et al., 2001; Bohm et al., 2004); the response is known to be mediated via CRTH2, because it is sensitive to blockade with CRTH2 antagonists (Bohm et al., 2004; Mathiesen et al., 2005; Mimura et al., 2005). Our study confirmed the inhibitive effect of ramatroban, which led to concentration-dependent dextral shifts of the PGD₂-mediated shape change responses, consistent with classic competitive antagonism (Fig. 7). TM30642 displayed the same antagonistic profile as ramatroban, primarily affecting the high-potency component of the biphasic dose-response curve. In contrast, TM30643 and TM30089 exhibited insurmountable antagonism with clear concentration-dependent suppressions of PGD₂ responses, albeit the nature of their insurmountable inhibition seemed to differ in the eosinophil ex vivo system; whereas TM30643 reduces both potency and efficacy of PGD₂, TM30089 seems to exclusively reduce the maximum responses of both components. We have previously reported that some aspects of CRTH2 signaling apparently occur independent of G protein activation (Mathiesen et al., 2005) and that both G protein-dependent and -independent signaling account for the characteristic shape change response of human eosinophils exposed to PGD₂. Thus, it is conceivable that the antagonists differentially inhibit the two components of the shape change response. At present, however, it is not possible to predict the consequences of such preferential inhibition for interference with eosinophil function in vivo. It is noteworthy that inhibition of PGD₂-mediated shape change was specifically mediated through blockade of CRTH2 because neither antagonist interfered with eosinophil shape change elicited by the chemokine eotaxin (CCL11), which acts through the chemokine CCR3 receptor (Supplemental Fig. 4; Bohm et al., 2004).

Molecular Mechanism of Insurmountable Antagonism

Insurmountable Antagonists Do Not Decrease CRTH2 Receptor Cell Surface Expression. To investigate a potential link between insurmountable antagonism and the ability of the compounds to internalize receptors, we analyzed CRTH2 cell surface expression in the absence and presence of different concentrations of antagonists (20, 200, and 2000 nM) in HEK293 cells stably expressing CRTH2. ELISA assays showed that none of the antagonists signifi-

cantly decreased CRTH2 cell surface numbers as opposed to PGD₂ (data not shown). This finding together with the effects of the antagonists on [³H]PGD₂ B_{max} in saturation and homologous competition binding analyses is congruent with the notion that insurmountability is not merely related to the disappearance of CRTH2 cell surface receptors but that antagonists rather make CRTH2 inaccessible to its agonist PGD₂.

Is Insurmountable Antagonism Mediated via an Allosteric Binding Site? To determine whether the insurmountable antagonism of PGD₂ by TM30089 and TM30643 observed in the functional assays could be because of the compounds interacting with an allosteric site different from the orthosteric PGD₂ binding domain, CRTH2-HEK293 cells were incubated with 3 nM [³H]PGD₂ until equilibrium was reached. Subsequently, dissociation of bound radioligand was monitored over time by adding an excess of unlabeled PGD₂ ($1000 \times K_D$) to prevent radioligand reassociation, in the

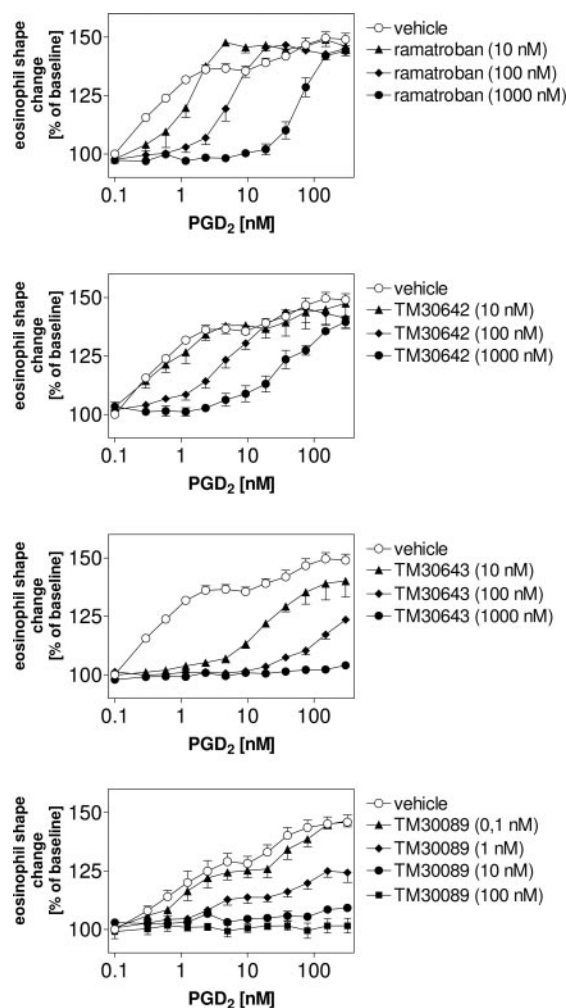


Fig. 7. Inhibition by ramatroban and the analogs TM30642, TM30643, and TM30089 of flow cytometric shape change responses of eosinophils exposed to PGD₂. Samples of polymorphonuclear leukocytes were pretreated with the antagonists or their vehicle for 30 min and then stimulated with PGD₂. Eosinophils were identified according to their autofluorescence, and shape change responses were quantified as percentage of the maximal response to PGD₂ in the absence of an antagonist. Although ramatroban and TM30642 shifted the concentration-response curve to PGD₂ rightward in a parallel manner, TM30643 and TM30089 induced both affinity shifts and depression of maximal efficacy of PGD₂ dose-response curves. Data are shown as mean \pm S.E., $n = 3$.

absence or presence of a high concentration of insurmountable antagonist. If the dissociation rate of [^3H]PGD2 is altered by the simultaneous presence of an antagonist, it must be because of antagonist interacting with an allosteric site distinct from the PGD2 binding domain. Figure 8A shows that none of the tested antagonists was capable of affecting the dissociation rate of [^3H]PGD2, in contrast to the positive control compound TM27868, which has recently been shown to significantly delay [^3H]PGD2 dissociation from CRTH2 receptors (Mathiesen et al., 2005). In another set of kinetic experiments, we tested whether [^3H]PGD2 dissociation was differentially affected when monitored only in the presence of excess PGD2, surmountable or insurmountable antagonists. To this end, CRTH2-HEK293 cells were incubated with [^3H]PGD2 until equilibrium was reached and dissociation was monitored over time by adding either a large excess of PGD2 (10 μM) or surmountable (20 μM ramatroban) or insurmountable (20 μM TM30089) ligand. Under these experimental conditions, acceleration or retardation of [^3H]PGD2 dissociation could be indicative of a cooperative mechanism of binding, whereas dissociation coinciding with that induced by PGD2 would indicate action via the orthosteric site. Dissociation of [^3H]PGD2, however, was essentially unchanged when reassociation was precluded by excess PGD2, ramatroban, or TM30089, respectively. Together, the different sets of kinetic experiments clearly support the notion that insurmountability of the antagonists does not arise from cooperative or allosteric interactions with CRTH2, occupation of which may lead to a conformational change refractory to agonist activation.

Relative Rates of Antagonist Dissociation Are Significantly Different for Surmountable and Insurmountable Ligands. To investigate whether insurmountability of TM30643 and TM30089 was related to slow dissociation from CRTH2, an indirect nonequilibrium method was used (Chris-

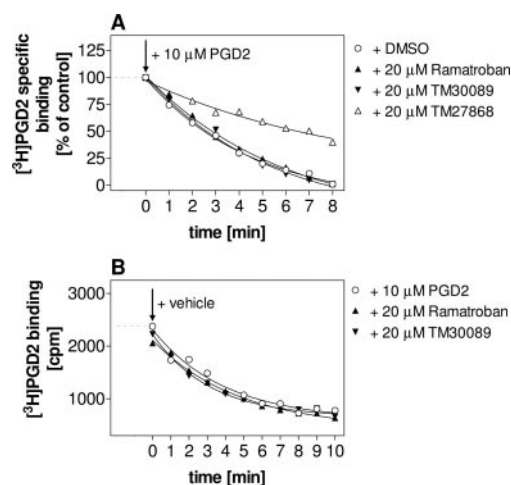


Fig. 8. Time course of [^3H]PGD2 dissociation from human CRTH2 receptors stably expressed in HEK293 cells. A, CRTH2-HEK293 whole cells were incubated with 4 nM [^3H]PGD2 for 60 min at 4°C until binding equilibrium was attained. Dissociation of [^3H]PGD2 was initiated by adding a large excess of PGD2 (10 μM) in the absence or presence of the indicated compounds. Nonspecific binding was determined in the presence of 10 μM PGD2. Binding levels after the initial equilibration phase were set 100% for all dissociation data sets. Shown are representative experiments performed as single point determinations. Two additional experiments gave similar results. B, dissociation was initiated by adding either the surmountable antagonist ramatroban or the insurmountable antagonist TM30089. Shown is a representative experiment.

topoulos et al., 1999; Verheijen et al., 2002) because none of the compounds are available in radiolabeled form. The method is based on the assumption that the degree of insurmountability correlates to the rate of antagonist dissociation. First, CRTH2-HEK293 whole cells were pre-exposed for 30 min with equivalent antagonist concentrations ($\sim 10 \times K_i$, which corresponds to approximately 90% receptor occupancy) followed by removal of unbound antagonist through a washing procedure. Subsequently, the rate of [^3H]PGD2 association was monitored over time (Fig. 9; Table 2). Assuming that the dissociation rate of the unlabeled antagonists will affect the association of the radioligand, apparent [^3H]PGD2 association rate constants can be computed to obtain a relative measure of antagonist dissociation. Association curves of [^3H]PGD2 in both absence and presence of antagonists were complex and best described by a two-component model ($F < 0.05$) as is the case for many radioligand agonists, which differentially interact with G protein-coupled and uncoupled forms of the receptor. As depicted in Fig. 9, the initial fast phase K_{app1} of [^3H]PGD2 association ($K_{app1} = 3.01 \pm 0.76 \text{ min}^{-1}$) ($t_{1/2} = 0.231 \text{ min}$; $n = 4$) was not significantly different across the various antagonist-pretreated groups and most probably reflects association of [^3H]PGD2 with the population of free receptors (approximately 10% of the total receptor population is not bound to antagonist at $10 \times K_i$). However, the rate constant K_{app2} for the second slower phase of [^3H]PGD2 association to the receptor population initially occupied by unlabeled antagonist was differentially affected by surmountable and insurmountable antagonists, respectively. Whereas the surmountable antagonists ramatroban and TM30642 modulated K_{app2} of [^3H]PGD2 association only slightly, the insurmountable antagonists TM30643 and TM30089 caused a dramatic reduction of K_{app2} by $\sim 1.5 \times 10^6$ -fold (Table 2). Thus, the ability of the antagonists to slow [^3H]PGD2 association seems to be closely related to their degree of suppression of agonist responses in the functional assays.

Discussion

Approximately 15 years ago, the orally available, small molecule ramatroban was developed as a thromboxane A_2 receptor antagonist for clinical use in various cardiovascular, cerebrovascular, and pulmonary diseases, but it has only recently been discovered to also antagonize CRTH2 (Sugi-

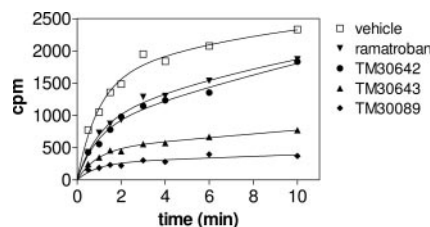


Fig. 9. Effects of ramatroban, TM30642, TM30643, and TM30089 on [^3H]PGD2 association kinetics in CRTH2-HEK293 cells. [^3H]PGD2 association kinetics were performed at 4°C in the presence of a single concentration of CRTH2 antagonist (chosen to correspond to $K_i \times 10$) or their vehicle (control). Cells were pre-exposed to the antagonists for 30 min at 4°C before [^3H]PGD2 association was initiated by ligand addition. [^3H]PGD2 association curves were analyzed by nonlinear regression analysis using a biexponential model as outlined in detail under *Materials and Methods*. Curves are representative of a single experiment. Four additional experiments gave similar results.

moto et al., 2003). We previously disclosed three ramatroban analogs that differ in structure only slightly from ramatroban (Fig. 1), yet exhibit very weak or no affinity for or functional activity on the thromboxane A_2 receptor, whereas their antagonistic activity on CRTH2 is preserved or potentiated (Ulven and Kostenis, 2005). In this study, we present a detailed pharmacological profile of these compounds and propose receptor binding modes to rationalize the observed pharmacological differences. All compounds inhibited PGD2 binding to CRTH2, but their nature of antagonism differed markedly (surmountable versus insurmountable). We were interested in exploring the molecular mechanisms underlying the experimental observations and also the structural features conferring insurmountability, because this is important from both a basic scientific and drug development point of view.

Proposed mechanisms for insurmountable antagonism include 1) slow dissociation of antagonist-receptor complexes; 2) interaction with allosteric binding sites inducing a conformational change in the receptor that compromises its interaction with the agonist; 3) antagonist-mediated conformational changes rendering receptors refractory to agonist stimulation; 4) antagonist-mediated desensitization or internalization; 5) slow antagonist removal from tissue compartments, cells, or matrix surrounding the receptor; 6) slowly interconverting receptor conformations; and 7) irreversible covalent ligand binding (for review, see Lew et al., 2000, Vauquelin et al., 2002).

Saturation and homologous inhibition binding experiments in the presence of the CRTH2 antagonists performed in this study indicated that TM30643 and TM30089 lead to a decrease of CRTH2 receptors capable of binding ligand; this pattern of behavior is also manifested in the functional effects of these antagonists (Figs. 3–7). It is now well established that receptor desensitization and internalization can occur in the absence of receptor activation (Whistler et al., 2002), and several examples of GPCRs undergoing antagonist-mediated internalization have been described previously (Perry et al., 2005). We therefore investigated whether insurmountable inhibition of PGD2 responses by the ramatroban analogs TM30089 and TM30643 was because of such a property. Although binding analyses indicated that the two insurmountable antagonists significantly depressed B_{max} , ELISA assays (data not shown) revealed that the total number of CRTH2 receptors on the cell surface was not reduced in their presence. Insurmountable antagonism of the compounds is therefore independent of receptor internalization.

To ascertain whether the insurmountability of the com-

pounds reflected a noncompetitive mechanism that was possibly mediated through an allosteric site, [3 H]PGD2 dissociation kinetic studies were performed. Occupation by the compounds of an allosteric site may lead to a conformational change of CRTH2 that may perturb its interaction with PGD2 itself and hence its ability to elicit a cellular response. The dissociation kinetics presented in Fig. 8, however, imply that it is unlikely that the insurmountable antagonists interact with an allosteric site, because neither compound altered the rate of [3 H]PGD2 dissociation from CRTH2 receptors (Fig. 8A). Furthermore, when dissociation of [3 H]PGD2 was monitored in the presence of excess PGD2, ramatroban, or TM30089 alone, the [3 H]PGD2 dissociation curves coincided for all three ligands, again suggesting interaction with a common binding site (Fig. 8B). Allosterically acting compounds, on the other hand, could have caused an acceleration or retardation of radioligand dissociation under these conditions because of cooperative binding.

Another possible explanation for insurmountability of orthosteric antagonists is the longevity of antagonist-receptor complexes caused by slow dissociation of antagonists from the receptors (Lew et al., 2000; Vauquelin et al., 2002). As outlined in the Appendix, binding behavior that is consistent with that observed in our current study can arise when the kinetics of one orthosteric ligand in the presence of another are so slow that insufficient readjustment of receptor occupancy occurs over the time course of the experiment. This phenomenon has previously been described as the “hemi-equilibrium” condition (Paton and Rang, 1966; Kenakin, 1997). Because a true state of equilibrium may not be practically reached during the course of such an experiment, affinity estimates for the antagonists have to be obtained under nonequilibrium conditions and hence are likely to deviate from the true affinities of the antagonists. However, as outlined in the Appendix, use of very low radioligand concentrations relative to its dissociation constant is a means to circumvent this problem. In fact, the lower the radioligand concentration used for competition binding assays, the closer will the apparent estimate of orthosteric antagonist affinity approach its true affinity, irrespective of whether antagonism is surmountable or insurmountable (shown by curve simulations in the Appendix). It is clear, however, that the drawback of using low radioligand concentrations is the introduction of uncertainty to the data because of a potentially low signal-to-noise ratio. In our study (Fig. 2; Table 1), the signal-to-noise ratio at low radioligand concentrations did not

TABLE 2

Rate constants and half-lives for [3 H]PGD2 association to CRTH2 receptors in the absence (vehicle) and presence of CRTH2 antagonists

[3 H]PGD2 association was measured in whole CRTH2-HEK293 cells pre-exposed for 30 min to vehicle or the various CRTH2 antagonists at equieffective concentrations ($10 \times K_i$). Data were fitted to the equation $Y = Y_{max1} \times (1 - e^{-K_{app1} \times X}) + Y_{max2} \times (1 - e^{-K_{app2} \times X})$ using Prism 4.03. K_{app1} and K_{app2} denote the rate constants for the first and second phase, respectively, of [3 H]PGD2 association. Association datasets in the presence of the antagonists were best described by keeping K_{app1} constant (K_{app1} amounted to $3.01 \pm 0.76 \text{ min}^{-1}$ ($t_{1/2} = 0.231 \text{ min}$) and was not significantly different across the antagonist-treated groups), while keeping K_{app2} as a variable. Unpaired t tests showed that the K_{app2} values of ramatroban and TM30642 were significantly different from those of TM30643 and TM30089, respectively ($p < 0.0001$). Data are from four independent experiments, one experiment of which is shown in Fig. 9.

Pretreatment with	K_{app2}	$t_{1/2}$	-fold $t_{1/2}$ over Ramatroban
	min^{-1}	min	
Vehicle	0.228 ± 0.04	3.05	
Ramatroban	0.151 ± 0.03	4.60	1
TM30642	0.090 ± 0.02	7.72	1.68
TM30643	$1.027 \times 10^{-7} \pm 0.08 \times 10^{-7}$	6.75×10^6	1.47×10^6
TM30089	$0.975 \times 10^{-7} \pm 0.08 \times 10^{-7}$	7.11×10^6	1.55×10^6

represent an experimental obstacle because binding data were very clean even under these conditions.

To more directly confirm whether the molecular mode of interaction between TM30643 or TM30089 with CRTH2 reflects the formation of a long-lasting ligand-receptor complex, additional kinetic binding assays were performed. Because the CRTH2 antagonists are not available in radiolabeled form at present, we took advantage of an indirect method to quantify antagonist dissociation from CRTH2 receptors (Christopoulos et al., 1999; Verheijen et al., 2002). This method determines the delay of [³H]PGD₂ association in the presence of equivalent antagonist concentrations (with respect to receptor occupancy) in wash-out experiments with antagonist-pretreated cells. It is assumed that the delay of agonist association reflects the dissociation rate of the unlabeled compounds from the receptors such that long-lasting receptor occupancy is correlated to the delay of agonist association. Although the four CRTH2 antagonists have quite similar affinities for CRTH2, they differ strikingly from a kinetic point of view. Whereas the surmountable antagonists ramatroban and TM30642 delay PGD₂ association only slightly, the insurmountable ligands markedly decrease agonist association in a manner related to their ability to suppress maximal

PGD₂ responses in functional assays (Fig. 9; Table 2). It is intriguing to note that compounds whose only structural differences reside in the absence or presence of a methyl group and the absence or presence of a methylene unit in the carboxylic acid chain may display such strikingly different pharmacological profiles. The shorter carboxylic acid chain seems to be associated with insurmountable behavior, whereas the absence or presence of a methyl group at the sulfonamide had no consequence for the kinetic behavior of the compounds. Different modes of antagonism for structurally closely related molecules have also been observed for AT₁ receptor antagonists (compare losartan versus its active metabolite EXP3174 (Schambye et al., 1994); or SC-54629 versus SC-54628, which differ only by a single methyl group (Olins et al., 1995); and histamine H₁ antagonists [compare (*R*)- versus (*S*)-cetirizine; Gillard et al., 2002]).

It is well known that the degree of insurmountable antagonism is related to the level of receptor expression in a given cell. In our study, the extent of depression of maximal PGD₂ responses was inversely correlated to receptor expression such that insurmountability was most evident in eosinophil shape change assays with “physiological levels” of receptor expression but least evident in GTPγS assays with very high levels of CRTH2 expression. In addition, we noted a significant discrepancy between the concentrations of insurmountable antagonist required to depress B_{\max} in radioligand binding assays and the ability to depress E_{\max} in functional assays. This discrepancy was particularly evident for TM30643 and may reflect differences in both receptor reserve but also temperature in binding (4°C) and functional assays (37°C), because binding processes are significantly slower at lower temperatures, leading to apparent overestimation of potency for slowly dissociating ligands.

In conclusion, our study explored in detail the pharmacological profile of three structurally closely related ramatroban analogs that display high potency and selectivity for CRTH2. It also provided insight into the structural features required to elicit insurmountable antagonism and the underlying molecular mechanism showing that slow dissociation from the receptor is sufficient to explain the pharmacological behavior. To date, TM30643 and TM30089 are the only insurmountable CRTH2 antagonists reported in the literature. Yet, it is premature to conclude that slowly dissociating antagonists with the potential to produce long-lasting receptor blockade will be therapeutically advantageous in clinical settings. Although it is clear that many additional pharmacokinetic factors govern duration of compound action in vivo, insurmountability may contribute to this duration and may allow compounds to act much longer as would be predicted from their plasma half-lives.

Appendix

The standard analyses applied to the agonist-antagonist interaction assume that the measured response, be it binding or function, reflects an equilibrium interaction between the ligands. If this assumption is not met by the experimental conditions, complex behaviors can be observed in the data that may lead the investigator to misinterpret the mechanism underlying the interaction. To explore some of the con-

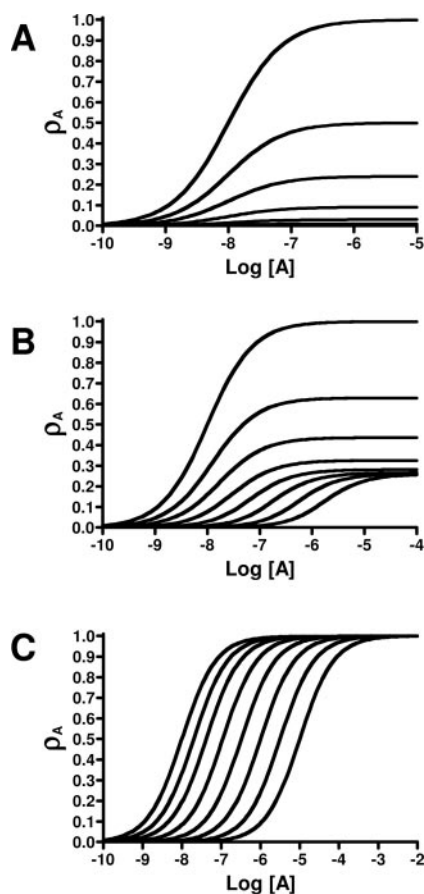


Fig. 10. Simulations of the interaction between an orthosteric ligand, A, in the absence (leftmost curve) or presence of a slowly dissociating orthosteric ligand, B, according to eq. 10. For all simulations, the following parameters were used: $K_A = 10^{-8}$ M, $K_B = 10^{-9}$ M, and $k_{\text{off}} = 10^{-4}$ s⁻¹. Concentrations of B ranged from 10^{-9} M to 10^{-7} M in half-log units. The incubation times were 0.5 s (A), 3000 s (B), and 100,000 s (equilibrium) (C). Ordinates, fractional occupancy of ligand A (ρ_A); abscissa, concentration of ligand A.

sequences of lack of appropriate equilibration between two orthosteric ligands, the following equation was used to simulate the re-adjustment in receptor occupancy between an orthosteric ligand, A, exposed to a receptor that has been pre-equilibrated with a second orthosteric ligand, B, as a function of time, t (Paton and Rang, 1966; Kenakin, 1997).

$$Y = \frac{[A]/K_A}{1 + [A]/K_A} \cdot \left(1 - \left(\frac{[B]/K_B}{1 + [A]/K_A + [B]/K_B} \right) \cdot \left[1 - e^{-k_{\text{off}} \cdot \left[\frac{1 + [A]/K_A + [B]/K_B}{1 + [A]/K_A} \right] \cdot t} \right] + \frac{[B]/K_B}{1 + [B]/K_B} \cdot e^{-k_{\text{off}} \left[1 + \frac{[A]/K_A + [B]/K_B}{1 + [A]/K_A} \right] \cdot t} \right) \quad (\text{A1})$$

where Y denotes the fractional occupancy of A; K_A and K_B denote the equilibrium dissociation constants of A and B, respectively; and k_{off} denotes the dissociation rate constant of B. Figure 11 illustrates the effects of varying the time of ligand interaction on the occupancy by A. If ligand B has a very low dissociation rate constant (Fig. 10A), it can be seen that at very short exposure times for A, there will be minimal readjustment of receptor occupancy; the occupancy profile of

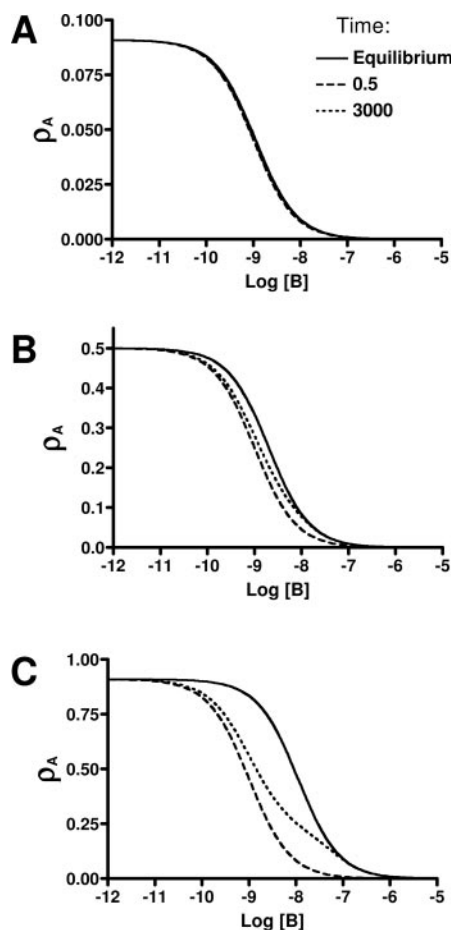


Fig. 11. Simulations of the interaction between a fixed concentration of orthosteric ligand, A, in the absence or presence of increasing concentrations of a slowly dissociating orthosteric ligand, B, according to eq. 10. Parameter values were as described for Fig. 10. Incubation times are indicated in the figure. The concentrations of ligand A were $0.1 \times K_A$ (A), $1 \times K_A$ (B), or $10 \times K_A$ (C). Ordinates, fractional occupancy of ligand A (ρ_A); abscissa, concentration of ligand B.

ligand A will essentially reflect its interaction only with the unoccupied receptors. Under this condition, the interaction is indistinguishable from a pure noncompetitive interaction where the effect of the presence of ligand B is to progressively reduce the maximal number of binding sites recognized by ligand A without affecting the affinity of the latter. As the incubation time is increased, a partial re-equilibration occurs that is characterized by a saturable depression in the maximal occupancy of A accompanied by a dextral displacement of the concentration-occupancy curve (Fig. 10B); this has previously been defined as a hemi-equilibrium condition (Paton and Rang, 1966; Kenakin, 1997; Christopoulos et al., 1999). Given sufficient time, complete re-equilibration occurs, and the characteristic features of a simple orthosteric interaction, namely, a parallel dextral shift of the concentration-occupancy curve of A in the presence of B with no effect on the maximal occupancy of A, is observed (Fig. 10C).

A more common method that is used experimentally to monitor the fractional occupancy of one ligand in the presence of another is the inhibition binding assay. Figure 11 shows a series of simulations based on this type of paradigm whereby the concentration of ligand A is held constant, and the effects on its fractional occupancy are monitored as the concentration of ligand B is increased. At a concentration of A that is 10-fold less (Fig. 11A) or equal to (Fig. 11B), its K_A value, it can be seen that no, or minimal, discrepancy occurs in the estimate of the affinity of ligand B. In contrast, at a concentration that is 10 times above the K_A , a dramatic effect of incubation time is evident on the location and shape of the inhibition binding curve. These latter simulations are particularly useful, because they indicate that the most accurate estimates of affinity for a slowly reversible orthosteric ligand are obtained by using as low a concentration as possible of the orthosteric probe ligand.

Acknowledgments

We are grateful to Helle Z. Andresen for excellent technical assistance, to Kate Hansen for excellent cloning support, and to Anders Heding (7TM Pharma A/S) for development of the improved BRET² assay using the GFP²- β -arr2, R393E, R395E mutant.

References

- Aramori I, Zenkoff J, Morikawa N, O'Donnell N, Asano M, Nakamura K, Iwami M, Kojo H, and Notsu Y (1997) Novel subtype-selective nonpeptide bradykinin receptor antagonists FR167344 and FR173657. *Mol Pharmacol* **51**:171-176.
- Bohm E, Sturm GJ, Weiglhofer I, Sandig H, Shichijo M, McNamee A, Pease JE, Kollrosier M, Peskar BA, and Heinemann A (2004) 11-Dehydro-thromboxane B2, a stable thromboxane metabolite, is a full agonist of chemoattractant receptor-homologous molecule expressed on TH2 cells (CRTH2) in human eosinophils and basophils. *J Biol Chem* **279**:7663-7670.
- Boie Y, Sawyer N, Slipetz DM, Metters KM, and Abramovitz M (1995) Molecular cloning and characterization of the human prostanoid DP receptor. *J Biol Chem* **270**:18910-18916.
- Carroll FY, Stolle A, Beart PM, Voerste A, Brabet I, Mauler F, Joly C, Antonicek H, Bockaert J, Muller T, et al. (2001) BAY36-7620: a potent non-competitive mGlu1 receptor antagonist with inverse agonist activity. *Mol Pharmacol* **59**:965-973.
- Christopoulos A, Parsons AM, Lew MJ, and El-Fakahany EE (1999) The assessment of antagonist potency under conditions of transient response kinetics. *Eur J Pharmacol* **382**:217-227.
- Gillard M, Van der PC, Moguelevsky N, Massingham R, and Chatelain P (2002) Binding characteristics of cetirizine and levocetirizine to human h(1) histamine receptors: contribution of Lys(191) and Thr(194). *Mol Pharmacol* **61**:391-399.
- Gonzalo J, Qiu Y, Coyle AJ, Hodge MR, and Cambridge MA (2005) CRTH2 (DP2), and not the DP1 receptor mediate allergen induced mucus production and airway hyperresponsiveness. The 2005 International Conference of the American Thoracic Society; 2005 May 20-25; San Diego, CA. Poster L41. Available at http://www.abstracts2view.com/ats05/view.php?nu=ATS5L_4220.
- Hata AN and Breyer RM (2004) Pharmacology and signaling of prostaglandin receptors: multiple roles in inflammation and immune modulation. *Pharmacol Ther* **103**:147-166.
- Heinemann A, Schuligoi R, Sabroe I, Hartnell A, and Peskar BA (2003) delta

- 12-Prostaglandin J₂, a plasma metabolite of prostaglandin D₂, causes eosinophil mobilization from the bone marrow and primes eosinophils for chemotaxis. *J Immunol* **170**:4752–4758.
- Hirai H, Tanaka K, Yoshie O, Ogawa K, Kenmotsu K, Takamori Y, Ichimasa M, Sugamura K, Nakamura M, Takano S, et al. (2001) Prostaglandin D₂ selectively induces chemotaxis in T helper type 2 cells, eosinophils and basophils via seven-transmembrane receptor CRTH2. *J Exp Med* **193**:255–261.
- Kenakin TP (1997) *Pharmacologic Analysis of Drug-Receptor Interaction*, 3rd ed. Lippincott-Raven, New York.
- Kostenis E, Martini L, Ellis J, Waldhoer M, Heydorn A, Rosenkilde MM, Norregaard PK, Jorgensen R, Whistler JL, and Milligan G (2005) A highly conserved glycine within linker I and the extreme C terminus of G protein α subunits interact cooperatively in switching G protein-coupled receptor-to-effector specificity. *J Pharmacol Exp Ther* **313**:78–87.
- Lew MJ, Ziovas J, and Christopoulos A (2000) Dynamic mechanisms of non-classical antagonism by competitive AT(1) receptor antagonists. *Trends Pharmacol Sci* **21**:376–381.
- March DR, Proctor LM, Stoermer MJ, Sbaglia R, Abbenante G, Reid RC, Woodruff TM, Wadi K, Paczkowski N, Tyndall JD, et al. (2004) Potent cyclic antagonists of the complement C5a receptor on human polymorphonuclear leukocytes. Relationships between structures and activity. *Mol Pharmacol* **65**:868–879.
- Marteau F, Le Poul E, Communi D, Communi D, Labouret C, Savi P, Boeynaems JM, and Gonzalez NS (2003) Pharmacological characterization of the human P2Y₁₃ receptor. *Mol Pharmacol* **64**:104–112.
- Mathiesen JM, Ulven T, Martini L, Gerlach LO, Heinemann A, and Kostenis E (2005) Identification of indole derivatives exclusively interfering with a G protein-independent signaling pathway of the prostaglandin D₂ receptor CRTH2. *Mol Pharmacol* **68**:393–402.
- Mimura H, Ikemura T, Kotera O, Sawada M, Tashiro S, Fuse E, Ueno K, Manabe H, Ohshima E, Karasawa A, et al. (2005) Inhibitory effect of the 4-aminotetrahydroquinoline derivatives, selective chemoattractant receptor-homologous molecule expressed on T helper 2 cell antagonists, on eosinophil migration induced by prostaglandin D₂. *J Pharmacol Exp Ther* **314**:244–251.
- Monneret G, Cossette C, Gravel S, Rokach J, and Powell WS (2003) 15R-Methyl-prostaglandin D₂ is a potent and selective CRTH2/DP₂ receptor agonist in human eosinophils. *J Pharmacol Exp Ther* **304**:349–355.
- Motulsky HJ and Christopoulos A (2004) *Fitting Models to Biological Data Using Linear and Nonlinear Regression. A Practical Guide to Curve Fitting*, Oxford University Press, New York.
- Nagata K, Tanaka K, Ogawa K, Kemmotsu K, Imai T, Yoshie O, Abe H, Tada K, Nakamura M, Sugamura K, et al. (1999) Selective expression of a novel surface molecule by human Th2 cells in vivo. *J Immunol* **162**:1278–1286.
- Olins GM, Chen ST, McMahon EG, Palomo MA, and Reitz DB (1995) Elucidation of the insurmountable nature of an angiotensin receptor antagonist, SC-54629. *Mol Pharmacol* **47**:115–120.
- Paton WDM and Rang HP (1966) A kinetic approach to the mechanism of drug action. *Adv Drug Res* **3**:57–80.
- Perry SJ, Junger S, Kohout TA, Hoare SR, Struthers RS, Grigoriadis DE, and Maki RA (2005) Distinct conformations of the corticotropin releasing factor type 1 receptor adopted following agonist and antagonist binding are differentially regulated. *J Biol Chem* **280**:11560–11568.
- Powell WS (2003) A novel PGD(2) receptor expressed in eosinophils. *Prostaglandins Leukot Essent Fatty Acids* **69**:179–185.
- Rashid M, Nakazawa M, and Nagatomo T (2003) Insurmountable antagonism of AT-1015, a 5-HT₂ antagonist, on serotonin-induced endothelium-dependent relaxation in porcine coronary artery. *J Pharm Pharmacol* **55**:827–832.
- Robarge MJ, Bom DC, Tumej LN, Varga N, Gleason E, Silver D, Song J, Murphy SM, Ekema G, Doucette C, et al. (2005) Isosteric ramatroban analogs: selective and potent CRTH-2 antagonists. *Bioorg Med Chem Lett* **15**:1749–1753.
- Schambye HT, Hjorth SA, Bergsma DJ, Sathe G, and Schwartz TW (1994) Differentiation between binding sites for angiotensin II and nonpeptide antagonists on the angiotensin II type 1 receptors. *Proc Natl Acad Sci USA* **91**:7046–7050.
- Shiraishi Y, Asano K, Nakajima T, Oguma T, Suzuki Y, Shiomi T, Sayama K, Niimi K, Wakaki M, Kagyo J, et al. (2005) Prostaglandin D₂-induced eosinophilic airway inflammation is mediated by CRTH2 receptor. *J Pharmacol Exp Ther* **312**:954–960.
- Soler D, Frank N, Zhu J, Fedyk E, Rose D, Coyle AJ, Hodge M, and Cambridge MA (2005) CRTH2 activates effector Th2 cell functions independently of antigen stimulation and costimulates proliferative responses via TCR activation. The 2005 International Conference of the American Thoracic Society; 2005 May 20–25; San Diego, CA. Poster L42. Available at http://www.abstracts2view.com/ats05/view.php?nu=AT55L_4974.
- Sugimoto H, Shichijo M, Iino T, Manabe Y, Watanabe A, Shimazaki M, Gantner F, and Bacon KB (2003) An orally bioavailable small molecule antagonist of CRTH2, ramatroban (BAY U3405), inhibits prostaglandin D₂-induced eosinophil migration in vitro. *J Pharmacol Exp Ther* **305**:347–352.
- Takezako T, Gogonea C, Saad Y, Noda K, and Karnik SS (2004) "Network leaning" as a mechanism of insurmountable antagonism of the angiotensin II type 1 receptor by non-peptide antagonists. *J Biol Chem* **279**:15248–15257.
- Tanaka K, Hirai H, Takano S, Nakamura M, and Nagata K (2004) Effects of prostaglandin D₂ on helper T cell functions. *Biochem Biophys Res Commun* **316**:1009–1014.
- Ulven T and Kostenis E (2005) Minor structural modifications convert the dual TP/CRTH2 antagonist ramatroban into a highly selective and potent CRTH2 antagonist. *J Med Chem* **48**:897–900.
- Vauquelin G, Van Liefde I, and Vanderheyden P (2002) Models and methods for studying insurmountable antagonism. *Trends Pharmacol Sci* **23**:514–518.
- Verheijen I, Vanderheyden PM, De Backer JP, Bottari S, and Vauquelin G (2002) Antagonist interaction with endogenous AT(1) receptors in human cell lines. *Biochem Pharmacol* **64**:1207–1214.
- Vrecl M, Jorgensen R, Pogacnik A, and Heding A (2004) Development of a BRET2 screening assay using beta-arrestin 2 mutants. *J Biomol Screen* **9**:322–333.
- Whistler JL, Gerber BO, Meng EC, Baranski TJ, von Zastrow M, and Bourne HR (2002) Constitutive activation and endocytosis of the complement factor 5a receptor: evidence for multiple activated conformations of a G protein-coupled receptor. *Traffic* **3**:866–877.

Address correspondence to: Dr. Evi Kostenis, 7TM Pharma A/S, Fremtidsvej 3, 2970 Hørsholm, Denmark. E-mail: ek@7tm.com
